NANO
LETTERS

XXXX
Vol. xx, No. x
-

Polymer Single-Nanowire Optical Sensors

Fuxing Gu,[†] Lei Zhang,[‡] Xuefeng Yin,[‡] and Limin Tong[†,*]

State Key Laboratory of Modern Optical Instrumentation, Department of Optical Engineering, and Institute of Microanalytical Systems, Department of Chemistry, Zhejiang University, Hangzhou 310027, China

Received April 30, 2008; Revised Manuscript Received June 16, 2008

ABSTRACT

We report highly versatile nanosensors using polymer single nanowires. On the basis of the optical response of waveguiding polymer single nanowires when exposed to specimens, functionalized polymer nanowires are used for humidity sensing with a response time of 30 ms and for NO_2 and NH_3 detection down to subparts-per-million level. The compact and flexible sensing scheme shown here may be attractive for very fast detection in physical, chemical, and biological applications with high sensitivity and small footprint.

Recently, one-dimensional nanostructures, such as nanowires, nanotubes, and nanofibers, have been attracting considerable attention in physical, chemical, and biological sensors due to their unique geometry with low dimension and large surface-to-volume ratio and their versatility for electrical and optical detection.[1−4] Polymer nanowires, inherited from the perm-selective nature and biocompatibility of polymer materials,[5] offer a number of highly attractive advantages for sensing applications. For example, gas molecules to be detected can be either selectively bound to their surface or diffused into the polymer matrix, which may be difficult for other materials such as semiconductor nanowires or glass nanofibers. Furthermore, polymers are hospitable to a variety of functional dopants ranging from metal oxides and fluorescent dyes to enzymes and are ready to offer plentiful choices for sensing schemes based on their favorable optical and electrical properties, as well as their mechanical flexibility, easy processing, and low cost.[5−7]

To date, polymer nanowires have been used to detect a variety of specimens including metal ions, toxic gases, and biotin-DNA.[4,8−11] Compared with the multiple-nanowire scheme that relies on the average response of many nanowires, single-nanowire detection presents special advantages of high sensitivity and fast response and may offer potentials for highly localized sensing with small footprint and high spatial resolution, as have been recently demonstrated in single-polymer-nanowire electrical sensors.[9−11] In contrast to electrical schemes, optical sensing offers potentials of high sensitivity, fast response, immunity to electromagnetic interference, and safe operation in explosive or combustive atmosphere, as well as more options for signal retrieval from optical intensity, spectrum, phase, polarization, and fluorescence lifetime.[12] However, to our knowledge, polymer single-nanowire optical sensors have not yet been reported. Here we demonstrate a simple and general approach to optical sensing using polymer single nanowires. Based on an evanescent coupling technique,[13] light is efficiently launched into and picked up from the nanowire using nanoscale fiber tapers (see Supporting Information). Polymer single-nanowire optical sensors are demonstrated for humidity and gas sensing with extraordinary fast response and high sensitivity.

Here polymer nanowires are fabricated by direct drawing of solvated polymers (see Supporting Information) that have been reported elsewhere.[14] To tailor the polymer nanowire for optical sensing, functional materials are doped into or blended with the solvated polymers before the drawing process. Functionalized polymer nanowires, including poly(methyl methacrylate) (PMMA), polystyrene (PS), polyacrylamide (PAM), and polyaniline/polystyrene (PANI/PS) nanowires, are obtained with minimum diameter less than 100 nm and lengths up to millimeters. As-fabricated polymer nanowires show smooth outer surface morphology without pronounced bending or obvious structural defects. For example, Figure 1a shows a scanning electron microscope (SEM) image of a typical 290-nm-diameter bromothymol blue (BTB)-doped PMMA nanowire. The excellent diameter uniformity and sidewall smoothness make the nanowire suitable for low-loss optical waveguiding and sensing.

Optical waveguiding in a single nanowire is implemented by an evanescent coupling method (see Supporting Information). As schematically illustrated in Figure 1b, a fiber taper drawn from a single-mode fiber with distal end about 500

* To whom correspondence should be addressed. E-mail: phytong@zju.edu.cn.
[†] State Key Laboratory of Modern Optical Instrumentation, Department of Optical Engineering.
[‡] Institute of Microanalytical Systems, Department of Chemistry.

10.1021/nl8012314 CCC: $40.75
Published on Web 08/02/2008

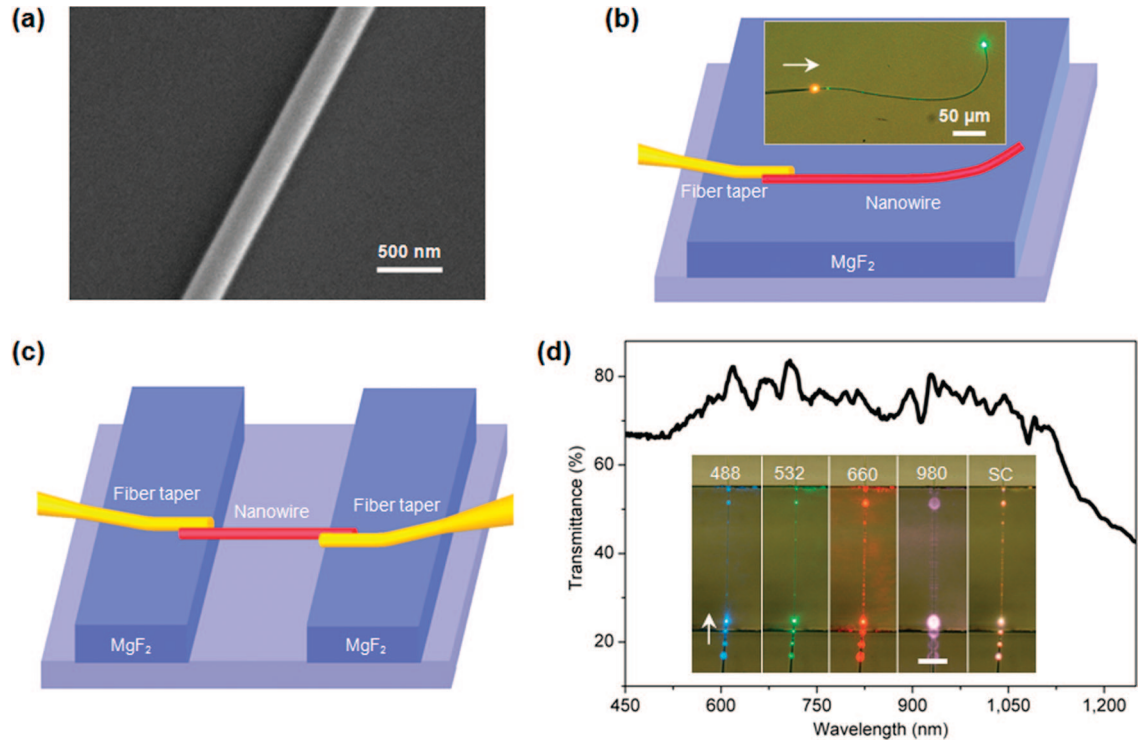

Figure 1. Characterization of polymer single nanowires. (a) SEM image of a 290-nm-diameter BTB-doped PMMA nanowire. (b) Schematic diagram of evanescent launching of a nanowire using a fiber taper. Inset, optical microscope image of the launching of a supercontinuum into a MgF_2-supported 440-nm-diameter PS nanowire using a fiber taper. (c) Schematic diagram of a microchannel-supported nanowire with two ends coupled with fiber tapers. (d) Broadband transmission spectrum of a 300-nm-diameter PMMA nanowire. The inset shows optical micrographs of the nanowire guiding a broadband supercontinuum (denoted as SC) and monochromatic lasers with wavelengths of 488, 532, 660, and 980 nm, respectively. Scale bar, 50 μm. The white arrows in b and d indicate the direction of light propagation.

nm in diameter is placed in parallel and close contact with one end of a polymer nanowire supported by a low-index substrate. Due to the strong evanescent coupling between the nanowire and the fiber taper, light can be efficiently launched into and picked up from the nanowire within a few micrometers' overlap.[15,16] When the whole nanowire is supported on the surface of the substrate, a short-pass filter effect that has been reported in semiconductor nanowires[17] is also observed in polymer nanowires. For reference, inset of Figure 1b shows a light from a broadband supercontinuum guided through a 440-nm-diameter PS nanowire (refractive index ~1.59) supported by a MgF_2 crystal (refractive index~1.39), an obvious "filtering effect" is observed at the output of the nanowire (orange light input vs green light output).

To adapt the nanowire for broadband waveguiding without obvious filtering effect, we support the nanowire using a microchannel, as schematically illustrated in Figure 1c. While the two ends of the nanowire are supported and coupled with fiber tapers on the surface of the substrate, the main part of the nanowire is suspended above the channel. Figure 1d characterizes the broadband transmission of a 300-nm-diameter PMMA nanowire (refractive index ~1.49), with optical micrographs of the nanowire guiding a broadband supercontinuum and monochromatic lasers (wavelengths of 488, 532, 660, and 980 nm, respectively) shown in the inset. The broadband transmittability of the nanowire is clearly seen. The channel-support configuration also makes it possible to guide light using thinner nanowires, which has been proved helpful to speed up the diffusion of specimen[9,11] and subsequently the response of the nanowire. At the wavelength far from the absorption band of the dopants, measured optical loss of the nanowire is typically lower than 0.1 dB/mm, which is neglectable due to the small effective length (e.g., less than 300 μm) of the nanowire used in this work.

To show optical sensing with single polymer nanowires, we first employ a PAM nanowire (drawn from a PAM aqueous solution) for relative humidity (RH) sensing based on a RH-dependent evanescent power leakage of a waveguiding nanowire. As shown in Figure 2a, a 410-nm-diameter 250-μm-length PAM nanowire is supported on a MgF_2 substrate sealed in a glass chamber and is optically connected to fiber tapers at both ends for evanescent coupling of the probing light. The coupling area is enclosed by a low-index fluoropolymer (refractive index ~1.38) to isolate it from the environment (see Supporting Information). Figure 2b shows the transmittance of the PAM nanowire exposed to atmosphere with RH from 35% to 88%, with an average cutoff wavelength around 545 nm due to the short-pass filter effect (see inset of Figure 1b). Before the cutoff point, the transmittance decreases monotonously with the increasing RH, which can be used for RH sensing. For reference, transmittances of the nanowire at 532 nm wavelength are provided in the inset of Figure 2b. The monotonous dependence can be explained as following: when exposed to high-RH atmosphere, the refractive index of the PAM nanowire (about 1.54) decreases as a result of the diffusion

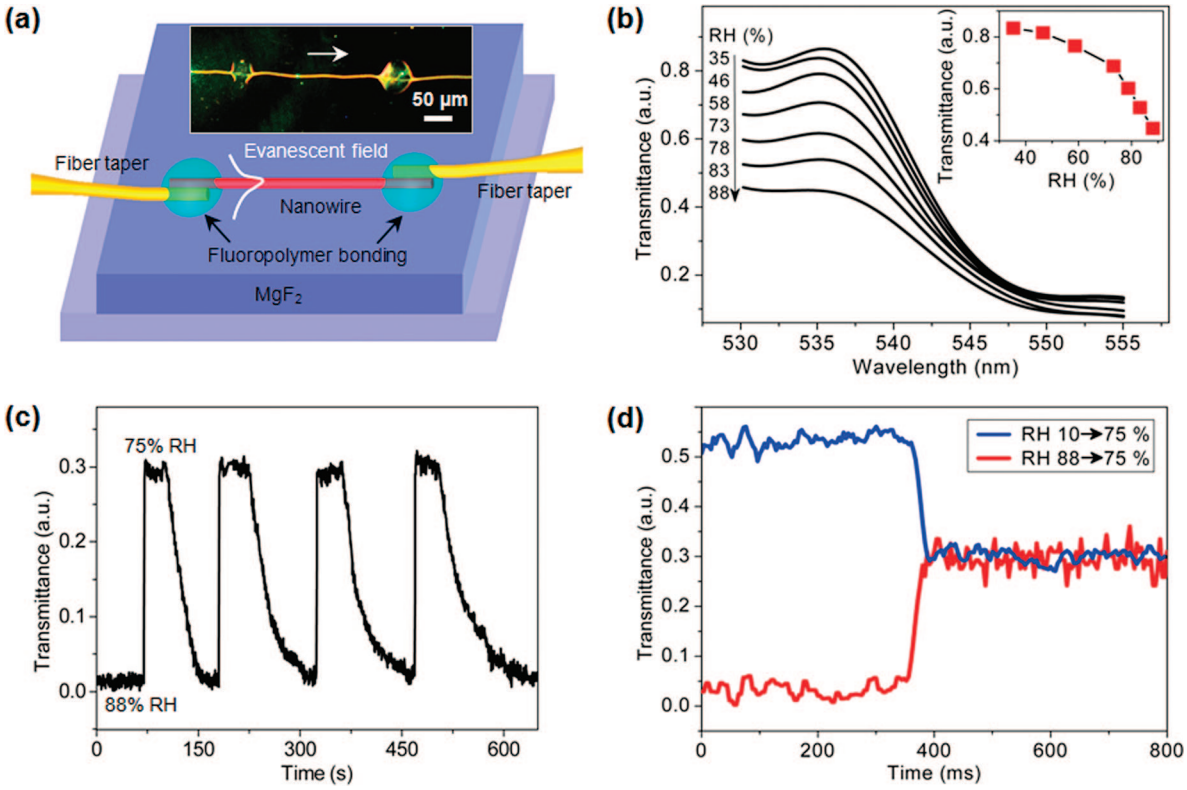

Figure 2. PAM single-nanowire humidity sensors. (a) Schematic illustration of the sensor. Inset, optical microscope image of a MgF_2-supported 410-nm-diameter PAM nanowire with a 532-nm-wavelength light launched from left side. The white arrow indicates the direction of light propagation. (b) Transmittance of a MgF_2-supported 410-nm-diameter PAM nanowire exposed to atmosphere of RH from 35% to 88%. Inset, transmittances of the nanowire at 532 nm wavelength. (c) Reversible response of the nanowire tested by alternately cycling 75% and 88% RH air. (d) Typical time-dependent transmittance of the sensor reveals the response time of about 24 ms when RH jumps from 10% to 75% and 30 ms when RH falls from 88% to 75%. The probing light are supercontinuum in b and 532-nm-wavelength laser in c and d.

of water molecules,[18] which leads to monotonous decrease in index contrast (between the nanowire and the substrate) and subsequently in optical confinement of the guided light. Meanwhile, light with longer wavelength tends to suffer higher evanescent leakage due to its higher fraction of evanescent waves, resulting in blue shift of the cutoff wavelength and higher leakage of the guided light nearby. Vice versa, a low-RH environment evaporates water inside the nanowire and increases the refractive index and transmittance of the nanowire. The reversible response of the nanowire is tested by alternately cycling 75% and 88% RH air inside the chamber, with an excellent reversibility shown in Figure 2c. The response time of the nanowire humid sensor is investigated by introduction of sudden changes of the humidity in the chamber, with typical time-dependent transmittance shown in Figure 2d. The estimated response time (baseline to 90% signal saturation) of the sensor is about 24 ms when RH jumps from 10% to 75% and 30 ms when RH falls from 88% to 75%, which are 1 or 2 orders of magnitude faster than those of existing RH sensors.[18−21] The remarkably fast response of the sensor can be attributed to the small diameter and large surface-to-volume ratio of the nanowire that enable rapid diffusion or evaporation of the water molecules, as well as fast signal retrieval using the optical approach.

When blended or doped with other functional materials, polymer nanowires can be used for optical sensing with high versatilities. For instance, here we employ a 250-nm-diameter PANI/PS nanowire for gas sensing (see Supporting Information). The nanowire is drawn from a polymer-blend solution of 2 wt % PANI doped with 10-camphorsulfonic and 5 wt % PS in chloroform and is suspended by a 250-μm-width MgF_2 microchannel and optically connected to fiber tapers at both ends (see Figure 1c). The sensor is operated by applying a nitrogen-diluted NO_2 gas onto the nanowire with a probing light of 532-nm wavelength. When exposed to NO_2, the increase of the oxidation degree of PANI results in spectral absorption at the wavelength of the probing light,[22] in which the absorbance is proportional to the degree of the oxidation that increases with the concentration of NO_2. Figure 3a shows a typical response of a 250-nm-diameter PANI/PS nanowire to 1 ppm NO_2. A clear absorbance is observed, with a response time of about 7 s, which is orders of magnitude faster than in other types of NO_2 sensors.[22−24] The time-dependent absorbance of the nanowire at room temperature to cyclic NO_2/nitrogen exposure with NO_2 concentration from 0.1 to 4 ppm is given in Figure 3b, indicating good reversibility of the nanowire response. The linear dependence of the absorbance over the NO_2 concentration (see inset) suggests that the PANI/PS nanowire could

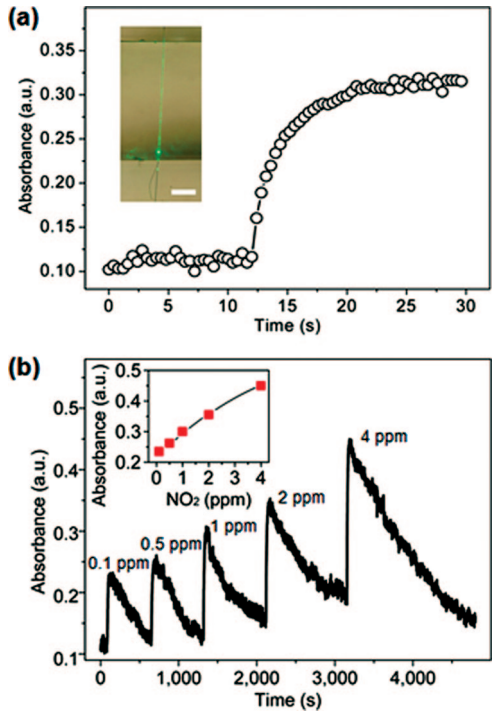

Figure 3. PANI/PS single-nanowire NO_2 sensors. (a) Optical response of a 250-nm-diameter PANI/PS nanowire to 1 ppm NO_2 with a 532-nm-wavelength light. Inset, a close-up optical micrograph of the sensing element with a 532-nm-wavelength probing light guided along the nanowire. Scale bar, 50 μm. (b) Time-dependent absorbance of the nanowire to cyclic NO_2/nitrogen exposure with NO_2 concentration from 0.1 to 4 ppm. Inset, dependence of the absorbance over the NO_2 concentration ranging from 0.1 to 4 ppm.

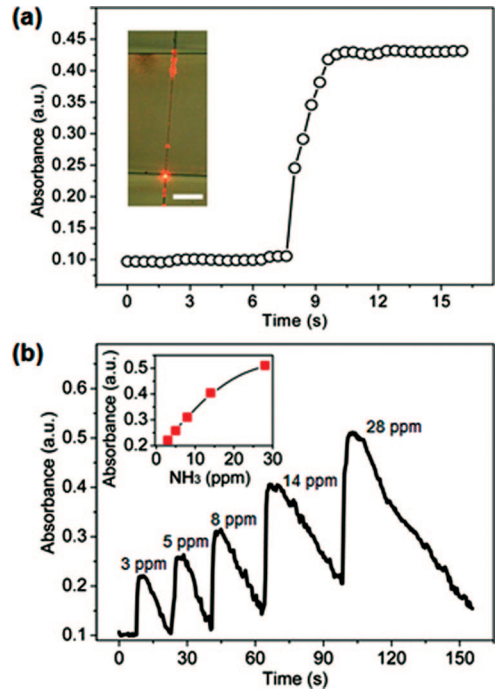

Figure 4. BTB-doped PMMA single-nanowire NH_3 sensors. (a) Optical response of a 270-nm-diameter BTB-doped PMMA nanowire to 14 ppm NH_3 with a 660-nm-wavelength light. Inset, a close-up optical micrograph of the sensing element with a 660-nm-wavelength probing light guided along the nanowire. Scale bar, 50 μm. (b) Time-dependent absorbance of the nanowire to NH_3 gas cycled with concentrations from 3 to 28 ppm. Inset, dependence of the absorbance over the NH_3 concentration ranging from 3 to 28 ppm.

function as a NO_2 optical sensor with a detection limit below 0.1 ppm.

Doping chemical indicators is another approach to activate the polymer nanowires for optical sensing. Here we demonstrate NH_3 gas sensing with a 270-nm-diameter BTB-doped PMMA nanowire, which is drawn from a chloroform solution containing 0.5 wt % BTB and 5 wt % PMMA. The nanowire is suspended by a 200-μm-width MgF_2 microchannel with a probing light of 660-nm wavelength. When a 14 ppm nitrogen-diluted NH_3 gas is introduced and diffuses into the nanowire, the BTB reacts with NH_3 and changes from acidic form to basic form, resulting in evident absorption of the probing light as shown in Figure 4a. The response time estimated from Figure 4a is about 1.8 s, which is much faster than in conventional ammonia sensors.[9,11,25,26] Figure 4b provides optical response of the nanowire to NH_3 gas cycled with concentrations from 3 to 28 ppm at room temperature, showing linear response (see inset) for NH_3 sensing below 14 ppm with good reversibility.

We have thus demonstrated a general approach to polymer single-nanowire optical sensors combining extraordinary faster response and high sensitivity. The use of a single nanowire for subwavelength-scale optical waveguiding not only bestows the sensor with a small footprint, fast response, and high sensitivity but also enables efficient coupling with outer fiber systems through fiber tapers. Since polymers are good hosts for a wide range of dopants and are easily functionalized by a number of techniques such as ionized gas treatments and UV irradiation,[27] polymer single-nanowire optical sensors for a variety of specimens can be realized on the basis of the above-mentioned optical detecting scheme. With recent advances in photonic applications of polymer single nanowires such as electroluminescent devices, [28] lasers,[29] and detectors,[30] the highly compact and flexible single-nanowire optical sensing scheme shown here may open up vast opportunities for very fast detection in physical, chemical, and biological applications with high sensitivity and small footprint.

Acknowledgment. This work was supported by the National Basic Research Programs of China (nos. 2007CB307003 and 2007CB714503) and the National Natural Science Foundation of China (no. 60425517). The authors thank Professor Hongzheng Chen and Dr. Fengna Xi for helpful discussions and Xu Liu, Xiaoyang Jiang, Qing Yang, Yuan Chen, and Zhifang Hu for their help in experiments.

Supporting Information Available: Nanowire fabrication, manipulation and processing; evanescent coupling between a polymer nanowire and a nanoscale fiber taper; light sources; nanowire enclosure with low-index UV curable fluoropolymer; methods for humidity and gas sensing. This material is available free of charge via the Internet at http://pubs.acs.org.

References

(1) Kong, J.; Franklin, N. R.; Zhou, C. W.; Chapline, M. G.; Peng, S.; Cho, K.; Dai, H. J. *Science* **2000**, *287*, 622–625.
(2) Cui, Y.; Wei, Q. Q.; Park, H. K.; Lieber, C. M. *Science* **2001**, *293*, 1289–1292.
(3) Comini, E.; Faglia, G.; Sberveglieri, G.; Pan, Z.; Wang, Z. L. *Appl. Phys. Lett.* **2002**, *81*, 1869–1871.
(4) Huang, J. X.; Virji, S.; Weiller, B. H.; Kaner, R. B. *J. Am. Chem. Soc.* **2003**, *125*, 314–315.
(5) Adhikari, B.; Majumdar, S. *Prog. Polym. Sci.* **2004**, *29*, 699–766.
(6) Li, D.; Xia, Y. N. *Adv. Mater.* **2004**, *16*, 1151–1170.
(7) Ma, H.; Jen, A. K.-Y.; Dalton, L. R. *Adv. Mater.* **2002**, *14*, 1339–1365.
(8) Wang, X. Y.; Drew, C.; Lee, S.; Senecal, K. J.; Kumar, J.; Samuelson, L. A. *Nano Lett.* **2002**, *2*, 1273–1275.
(9) Liu, H. Q.; Kameoka, J.; Czaplewski, D. A.; Craighead, H. G. *Nano Lett.* **2004**, *4*, 671–675.
(10) Ramanathan, K.; Bangar, M. A.; Yun, M.; Chen, W.; Myung, N. V.; Mulchandani, A. *J. Am. Chem. Soc.* **2005**, *127*, 496–497.
(11) Kemp, N. T.; McGrouther, D.; Cochrane, J. W.; Newbury, R. *Adv. Mater.* **2007**, *19*, 2634–2638.
(12) *Fiber Optical Sensors: An Introduction for Engineers and Scientists*; Udd, E., Ed.; Wiley: New York, 1991.
(13) Tong, L. M.; Gattass, R. R.; Ashcom, J. B.; He, S. L.; Lou, J. Y.; Shen, M. Y.; Maxwell, I.; Mazur, E. *Nature* **2003**, *426*, 816–819.
(14) Harfenist, S. A.; Cambron, S. D.; Nelson, E. W.; Berry, S. M.; Isham, A. W.; Crain, M. M.; Walsh, K. M.; Keynton, R. S.; Cohn, R. W. *Nano Lett.* **2004**, *4*, 1931–1937.
(15) Tong, L. M.; Lou, J. Y.; Gattass, R. R.; He, S. L.; Chen, X. W.; Liu, L.; Mazur, E. *Nano Lett.* **2005**, *5*, 259–262.
(16) Huang, K. J.; Yang, S. Y.; Tong, L. M. *Appl. Opt.* **2007**, *46*, 1429–1434.
(17) Law, M.; Sirbuly, D. J.; Johnson, J. C.; Goldberger, J.; Saykally, R. J.; Yang, P. D. *Science* **2004**, *305*, 1269–1273.
(18) Barry, R. A.; Wiltzius, P. *Langmuir* **2006**, *22*, 1369–1374.
(19) Matias, I. R.; Arregui, F. J.; Corres, J. M.; Bravo, J. *IEEE Sens. J.* **2007**, *7*, 89–95.
(20) Zhang, Y. S.; Yu, K.; Jiang, D. S.; Zhu, Z. Q.; Geng, H. R. *Appl. Surf. Sci.* **2005**, *242*, 212–217.
(21) Hernandez-Ramirez, F.; Tarancón, A.; Casals, O.; Arbiol, J.; Romano-Rodríguez, A.; Morante, J. R. *Sens. Actuators B* **2007**, *121*, 3–17.
(22) Elizalde-Torres, J.; Hu, H. L.; Garcia-Valenzuela, A. *Sens. Actuators, B* **2004**, *98*, 218–226.
(23) McAlpine, M. C.; Ahmad, H.; Wang, D. W.; Heath, J. R. *Nat. Mater.* **2007**, *6*, 379–384.
(24) Yan, X. B.; Han, Z. J.; Yang, Y.; Tay, B. K. *Sens. Actuators, B* **2007**, *123*, 107–113.
(25) Cao, W. Q.; Duan, Y. X. *Sens. Actuators, B* **2005**, *110*, 252–259.
(26) Tao, S. Q.; Xu, L.; Fanguy, J. C. *Sens. Actuators, B* **2006**, *115*, 158–163.
(27) Goddard, J. M.; Hotchkiss, J. H. *Prog. Polym. Sci.* **2007**, *32*, 698–725.
(28) Moran-Mirabal, J. M.; Slinker, J. D.; DeFranco, J. A.; Verbridge, S. S.; Ilic, R.; Flores-Torres, S.; Abruna, H.; Malliaras, G. G.; Craighead, H. G. *Nano Lett.* **2007**, *7*, 458–463.
(29) O'Carroll, D.; Lieberwirth, I.; Redmond, G. *Nat. Nanotechnol.* **2007**, *2*, 180–184.
(30) O'Brien, G. A.; Quinn, A. J.; Tanner, D. A.; Redmond, G. *Adv. Mater.* **2006**, *18*, 2379–2383.

NL8012314